Journal of Nuclear Medicine, published on September 4, 2020 as doi:10.2967/jnumed.120.248278

Treatment Monitoring of Immunotherapy and Targeted Therapy using ^{18}F-FET PET in Patients with Melanoma and Lung Cancer Brain Metastases: Initial Experiences

[1,2,3]Norbert Galldiks, [2,4]Diana S.Y. Abdulla, [2,4]Matthias Scheffler, [5]Fabian Wolpert, [1]Jan-Michael Werner, [6]Martin Hüllner, [3]Gabriele Stoffels, [2,7]Viola Schweinsberg, [2,7]Max Schlaak*, [2,7]Nicole Kreuzberg, [2,8]Jennifer Landsberg, [3,9]Philipp Lohmann, [1]Garry Ceccon, [2,10]Christian Baues, [2,10]Maike Trommer, [2,9]Eren Celik, [2,9]Maximilian I. Ruge, [3,9]Martin Kocher, [2,10]Simone Marnitz, [1,3]Gereon R. Fink, [11]Jörg-Christian Tonn, [5]Michael Weller, [3,12]Karl-Josef Langen, [2,4]Jürgen Wolf, and [2,7]Cornelia Mauch

[1]Dept. of Neurology, Faculty of Medicine and University Hospital Cologne, University of Cologne, Cologne, Germany

[2]Center of Integrated Oncology (CIO), Universities of Aachen, Bonn, Cologne, and Duesseldorf, Germany

[3]Inst. of Neuroscience and Medicine (INM-3, -4), Research Center Juelich, Juelich, Germany

[4]Lung Cancer Group, Dept. I of Internal Medicine, Faculty of Medicine and University Hospital Cologne, University of Cologne, Cologne, Germany

[5]Dept. of Neurology & Brain Tumor Center, University Hospital and University of Zurich, Zurich, Switzerland

[6]Dept. of Nuclear Medicine, University Hospital and University of Zurich, Zurich, Switzerland

[7]Dept. of Dermatology, Faculty of Medicine and University Hospital Cologne, University of Cologne, Cologne, Germany

[8]Dept. of Dermatology, University Hospital Bonn, Bonn, Germany

[9]Dept. of Stereotaxy and Functional Neurosurgery, Faculty of Medicine and University Hospital Cologne, University of Cologne, Cologne, Germany

[10]Dept. of Radiation Oncology, Faculty of Medicine and University Hospital Cologne, University of Cologne, Cologne, Germany

[11]Dept. of Neurosurgery, University Hospital LMU Munich, Munich, Germany

[12]Dept. of Nuclear Medicine, RWTH University Hospital Aachen, Aachen, Germany

*(*current address: Dept. of Dermatology and Allergy, University Hospital LMU Munich, Munich, Germany)*

Running title: ^{18}F-FET PET Monitoring of immunotherapy

Target journal: *Journal of Nuclear Medicine*

Correspondence:
Norbert Galldiks, MD
Institute of Neuroscience and Medicine (INM-3), Research Center Juelich, Leo-Brandt-St. 5, 52425 Juelich, Germany
Phone: +49-2461-61-9324, FAX: +49-2461-61-1518
Email: n.galldiks@fz-juelich.de

and Dept. of Neurology, University Hospital Cologne, Kerpener St. 62, 50937 Cologne, Germany
Phone: +49-221-478-86124, FAX: +49-221-478-5669
Email: norbert.galldiks@uk-koeln.de

Disclosure of Potential Conflicts of Interest

Related to the present work, the authors disclosed no potential conflicts of interest.

Funding

The Cologne Clinician Scientist-Program (CCSP) of the Deutsche Forschungsgemeinschaft (DFG, FI 773/15-1), Germany, supported this work.

Word count

All sections: 6,144

AUTHOR CONTRIBUTIONS

Study design: N.G.

Data acquisition: N.G, D.S.Y.A., M.S., F.W., M.H., G.S., V.S., N.K., J.L., P.L., G.C., J-M.W., C.B., M.T.-N.

Data analysis, writing of manuscript drafts: N.G., G.S., K-J.L.

Interpretation of data: N.G., F.W., K-J.L., J.W., C.M.

Revising manuscript, approving final content of manuscript: All.

ABSTRACT

Purpose: We investigated the value of O-(2-[^{18}F]fluoroethyl)-L-tyrosine (^{18}F-FET) PET for treatment monitoring of immune checkpoint inhibition (ICI) or targeted therapy (TT) alone or in combination with radiotherapy in patients with brain metastases (BM) since contrast-enhanced MRI often remains inconclusive.

Methods: We retrospectively identified 40 patients with 107 BM secondary to melanoma (n=29 with 75 BM) or non-small cell lung cancer (n=11 with 32 BM) treated with ICI or TT who had ^{18}F-FET PET (n=60 scans) for treatment monitoring from 2015-2019. The majority of patients (n=37; 92.5%) had radiotherapy during the course of disease. In 27 patients, ^{18}F-FET PET was used for the differentiation of treatment-related changes from BM relapse following ICI or TT. In 13 patients, ^{18}F-FET PET was performed for response assessement to ICI or TT using baseline and follow-up scans (median time between scans, 4.2 months). In all lesions, static and dynamic ^{18}F-FET PET parameters were obtained (i.e., mean tumor-to-brain ratios (TBR), time-to-peak values). Diagnostic accuracies of PET parameters were evaluated by receiver-operating-characteristic analyses using the clinical follow-up or neuropathological findings as reference.

Results: A TBR threshold of 1.95 differentiated BM relapse from treatment-related changes with an accuracy of 85% (P=0.003). Metabolic responders to ICI or TT on ^{18}F-FET PET had a significantly longer stable follow-up (threshold of TBR reduction relative to baseline, ≥10%; accuracy, 82%; P=0.004). Furthermore, at follow-up, time-to-peak values in metabolic responders increased significantly (P=0.019).

Conclusions: ^{18}F-FET PET may add valuable information for treatment monitoring in BM patients treated with ICI or TT.

KEYWORDS

checkpoint inhibitors; pseudoprogression; response assessment; treatment-related changes; radionecrosis

INTRODUCTION

Brain metastases (BM) develop in 20-40% of patients with late-stage cancer and are associated with a poor prognosis. Frequently used treatment options are radiosurgery, whole-brain radiation therapy, surgical resection in oligometastases, and systemic cytotoxic chemotherapy (*1*). The advent of immunotherapy using immune checkpoint inhibition (ICI) and targeted therapy (TT) has considerably improved the overall survival of cancer, particularly in patients with melanoma or lung cancer (*2-4*). Additionally, more recent trials have shown that patients with BM from melanoma or lung cancer may also benefit from these agents alone or in combination (*5-8*).

Following various newer treatment options for patients with BM such as immunotherapy using ICI or TT, imaging findings on contrast-enhanced anatomical MRI can be highly variable, especially when these agents are used in combination with radiotherapy, and the interpretation regarding the differentiation of treatment-related changes from BM relapse is often difficult (*9*). Additionally, this uncertainty may also negatively affect the assessment of response to these newer treatment options, particularly if applied in combination (e.g., ICI or TT plus radiotherapy) (*10*). For example, immunogenic reactions related to ICI may trigger inflammation and intratumoral infiltrates including cytotoxic T cells, thereby leading to MR imaging findings that suggest BM relapse. Correspondingly, histopathology typically shows inflammatory cells (*11*), but not mitotically active tumor cells. This is also aggravated by the fact that progressive imaging changes on anatomical MRI early after treatment initiation might represent an actual tumor progression that ultimately becomes controlled by a delayed immune response (*9*). Although the immunotherapy Response Assessment in Neuro-Oncology (iRANO)

Working Group recommended both clinical and standard MRI criteria to overcome the clinical problem of immunotherapy-related pseudoprogression (*9*), these newer treatment options seem to impose demands on brain imaging beyond those offered by routine anatomical MRI techniques.

Metabolic PET imaging may help to overcome some of these imaging challenges. Radiolabeled amino acids are of particular interest for brain tumor imaging using PET because of their increased uptake in neoplastic tissue but low uptake in normal brain parenchyma, resulting in an improved tumor-to-brain contrast compared to glucose PET (*12*). Importantly, a key feature of amino acid tracers is their ability to pass the intact blood-brain-barrier which allows the depiction of tumor tissue beyond contrast enhancement in MRI (*12*). Increased uptake of radiolabeled amino acids is related to amino acid transporters of the L type (LAT transporters), which are often overexpressed in brain tumors (*13,14*). LAT transporter overexpression in BM makes intracranial metastases also a compelling target for amino acid PET imaging (*15*). Moreover, the RANO group has analyzed the additional diagnostic value of amino acid PET in patients with glioma and BM and recommended the use of this imaging technique in addition to conventional MRI especially for the delineation of brain tumor extent, treatment response assessment, and the differentiation of treatment-related changes from tumor progression (*16-18*).

However, only little data is currently available for the evaluation of ICI- or TT-treated BM patients in combination without or with radiotherapy using amino acid PET. The purpose of the present study was to investigate the value of amino acid PET using O-(2-[^{18}F]fluoroethyl)-L-tyrosine (**^{18}**F-FET) as an additional imaging method compared with

conventional contrast-enhanced MRI alone for treatment monitoring in predominantly heavily pretreated patients with BM from melanoma or non-small cell lung cancer (NSCLC) treated with ICI or TT alone or in combination with radiotherapy.

PATIENTS AND METHODS

Patients

From 2015 to 2019, 40 adult patients with metastatic brain tumors secondary to histomolecularly defined malignant melanoma (MM; n=29) or non-small cell lung cancer (NSCLC; n=11) (mean age, 59 ± 13 years; range, 27-83 years; 8 women and 32 men) treated with ICI or TT who underwent in total 60 ^{18}F-FET PET scans for treatment monitoring were included in this retrospective study. All patients had at least one contrast-enhancing lesion (n=75 in MM patients, and n=32 in NSCLC patients; total number of contrast-enhancing lesions, n=107) on cerebral MRI. The majority of patients (n=37; 92.5%) had radiotherapy during the course of disease (Supplemental Tables 1-3).

Twenty-seven of these 40 patients with equivocal MRI findings following ICI, TT, radiotherapy, or combinations thereof were referred to the Research Center Juelich (n=18), Germany, or to the Brain Tumor Center of the University Hospital Zurich (n=9), Switzerland, to differentiate actual BM relapse from treatment-related changes using ^{18}F-FET PET (total number of ^{18}F-FET PET examinations, 32 scans). A detalied overview of the patients' pretreatment is listed in Supplemental Tables 1 and 2.

The remaining 13 patients were referred to the Research Center Juelich, Germany, for the evaluation of the treatment effects following ICI, TT, radiotherapy, or combinations thereof using ^{18}F-FET PET. In contrast to the other 27 patients, each of these patients

had a baseline scan and at least one follow-up scan (range, 1-2 scans) (median time between baseline and first follow-up scan, 4.2 months; total number of scans, 28). The applied therapy including the pretreatment before ^{18}F-FET PET imaging is listed in Supplemental Table 3.

The local ethics committees approved the retrospective analysis of the data. There was no conflict with the Declaration of Helsinki. All subjects had given written informed consent for the PET investigation.

Conventional MR Imaging

In accordance with the International Standardized Brain Tumor Imaging Protocol (BTIP) (*19*), MR imaging was performed using a 1.5 T or 3.0 T MRI scanner with a standard head coil before and after administration of a gadolinium-based contrast agent (0.1 mmol/kg body weight). The sequence protocol comprised at least 3D isovoxel T1-weighted, 2D T2-weighted, and 2D fluid-attenuated inversion recovery-weighted (FLAIR) sequences. MRI changes at first follow-up compared to the baseline scan were assigned according to the RANO criteria for BM (*20*).

Diagnosis of Treatment-related Changes and Evaluation of Treatment Response

In two cases tissue was available and treatment-related changes were diagnosed by prominent necrosis with no or only minimal identifiable tumor remnants in one case and the presence of viable tumor tissue confirmed BM relapse in the other case.

In the remaining patients, a neuropathological diagnosis was unavailable, and iRANO criteria (*9*) were considered for diagnostic assessment. According to the iRANO

criteria (*9*), treatment-related changes were assumed when (i) the lesions showed spontaneous shrinkage or remained stable in size on contrast-enhanced MRI during a follow-up of at least of 3 months (median follow-up, 7 months; range, 3-25 months); (ii) the clinical condition remained stable; (iii) and no new neurological symptoms occurred / neurological deficits remained unchanged.

Response to the applied treatment on ^{18}F-FET PET was considered if a decrease of metabolic activity at follow-up was associated with a stable clinical course for at least 6 months, i.e., the clinical condition remained stable or even improved, and no new neurological symptoms occurred, or existing neurological deficits remained unchanged, as documented in the patients' charts.

^{18}F-FET PET Imaging

The amino acid ^{18}F-FET was produced via nucleophilic ^{18}F-fluorination with a radiochemical purity of greater than 98%, specific radioactivity greater than 200 GBq/µmol, and a radiochemical yield of about 60% (*21*). According to international guidelines for brain tumor imaging using labeled amino acid analogues (*18*), patients fasted for at least 4 h before the PET measurements.

At the Research Center Juelich, Germany, all patients underwent a dynamic PET scan from 0 to 50 minutes post-injection of 3 MBq of ^{18}F-FET per kg of body weight. PET imaging was performed either on an ECAT Exact HR+ PET scanner in 3-dimensional mode (n= 19 patients; Siemens, Erlangen, Germany; axial field-of-view, 15.5 cm) or simultaneously with 3.0 T MR imaging using a BrainPET insert (n=12 patients; Siemens, Erlangen, Germany; axial field of view, 19.2 cm). The BrainPET is a compact cylinder that

fits into the bore of the Magnetom Trio MR scanner (*22*). Iterative reconstruction parameters were 16 subsets, 6 iterations using the OSEM algorithm for the ECAT HR+ PET scanner and two subsets, 32 iterations using the OP-OSEM algorithm for the BrainPET. Data were corrected for random, scattered coincidences, dead time, and motion, for both systems. Attenuation correction for the ECAT HR+ PET scan was based on a transmission scan, and for the BrainPET scan on a template-based approach (*22*). The reconstructed dynamic data sets consisted of 16 time frames (5 x 1 minute; 5 x 3 min; 6 x 5 minutes) for both scanners.

At the Dept. of Nuclear Medicine of the University Hospital Zurich, Switzerland, ^{18}F-FET PET images were acquired on a PET/CT scanner (Discovery 690 Standard, GE Healthcare, Waukesha (WI), USA; n=4 patients) or on a PET/MR (3.0 T) scanner (Signa PET/MR, GE Healthcare, Waukesha (WI), USA; n=5 patients). Patients were injected with a standardized dose of 130 MBq 20 minutes before (PET/CT) or immediately before (PET/MR) the dynamic PET acquisition. All PET images were reconstructed using the OSEM-algorithm in conjunction with point spread function modelling. The reconstructed dynamic data sets consisted of 8 time frames (8 x 5 minutes) for the PET/MR scanner, and 4 time frames (4 x 5 minutes) for the PET/CT scanner.

^{18}F-FET PET Data Analysis

^{18}F-FET uptake in the tissue was expressed as standardized uptake value (SUV) by dividing the radioactivity (kBq/mL) in the tissue by the radioactivity injected per gram of bodyweight. All PET and MR images were co-registered and fusion results were inspected and, if necessary, adapted based on anatomical landmarks. For the evaluation of ^{18}F-FET

data, summed PET images over 20-40 minutes post-injection were used. Mean tumoral ^{18}F-FET uptake was determined by a two-dimensional auto-contouring process using a tumor-to-brain ratio (TBR) at a threshold of 1.6 (*18,23,24*). Mean TBRs (TBR_{mean}) were calculated by dividing the mean SUV of the tumor ROI by the mean SUV of a larger reference ROI placed in the semioval center of the contralateral unaffected hemisphere including white and grey matter (*18,24,25*). In the case of multiple brain metastases, ROI analyses for TBR_{mean} calculation were performed for each metastasis separately. Due to the use of different PET scanners (n=4) in two centers, calculations of maximum TBR values (TBR_{max}) were not obtained, because TBR_{max} values may vary considerably (*26*) and the comparability may be affected by the different spatial resolution of the PET scanners.

At the Research Center Juelich, time-activity curves (TACs) of ^{18}F-FET uptake (mean SUV) in the tumor were generated by the application of a spherical volume-of-interest (VOI) with a volume of 2 mL centred on the voxel with the maximum tumor uptake (*27*) and the reference ROI as described above to the entire dynamic dataset. A reference TAC was generated by placing a reference ROI in the unaffected brain tissue as reported (*27*). For TAC evaluation, the time-to-peak (TTP; time in minutes from the beginning of the dynamic acquisition up to the maximum SUV of the lesion) was determined. Due to the different dynamic ^{18}F-FET PET acquisition protocol used in the 9 patients from the Dept. of Nuclear Medicine of the University Hospital Zurich, Switzerland, a TAC evaluation by TTP values in these 9 patients was not performed.

Statistical Analyses

Descriptive statistics are provided as mean and standard deviation and/or median and range. The Student's t-test was used to compare two groups. The Mann-Whitney rank-sum test was used when variables were not normally distributed. The change of TTP values in the same patients were compared using the paired t-test.

The diagnostic performance of TBR_{mean} for the differentiation of BM relapse from treatment-related changes was assessed by receiver operating characteristic (ROC) curve analyses using histological confirmation or clinical course as reference. In the case of multiple BM, the lesion with the highest metabolic activity was selected for the ROC analysis.

To determine the optimal threshold of TBR_{mean} to identify responding patients to ICI, TT, radiotherapy, or combinations thereof, a ROC analysis was calculated using a stable clinical course of 6 months as reference. The lesion with the highest metabolic activity was selected for response assessment, i.e., relative TBR_{mean} changes during follow-up relative to baseline. Furthermore, the lesion with the highest metabolic activity was selected for TTP calculation.

As a measure of the test's diagnostic quality, the area under the ROC curve (AUC), its standard error, and level of significance were determined. Decision cut-off was considered optimal when the product of paired values for sensitivity and specificity reached its maximum. The diagnostic performance of TBR_{mean} in combination with the

corresponding TTP value was evaluated by the Fisher exact test for 2 × 2 contingency tables.

P-values of 0.05 or less were considered significant. Statistical analyses were performed using SPSS statistics (Release 26.0, SPSS Inc., Chicago, IL, USA).

RESULTS

Targeted and Checkpoint Inhibitor Therapy in Relation to Radiotherapy

The majority of patients (n=37; 92.5%) had radiotherapy during the course of disease. Prior to ^{18}F-FET PET imaging, 70% of the patients (n=28) had undergone radiotherapy, either as single modality (35%; n=14) or in combination with ICI or TT (35%; n=14). Radiosurgery was the most frequent used radiotherapy modality (60%, range of surface radiation dose, 16-25 Gy/50-80% isodose level) (Supplemental Table 1).

Diagnosis of Recurrent Brain Metastases and Treatment-related Changes

Following multimodal treatment including radiotherapy, ICI, TT, and combinations thereof (Supplemental Table 1, 2), treatment-related changes were diagnosed in 17 patients. This was based on stable neurological symptoms and no significant enlargement of the lesion on further follow-up MR images after a median of 7 months (range, 3-25 months) in 16 patients, or on neuropathology in one patient. In total, recurrent BM were diagnosed in 10 patients. Based on the deterioration of the clinical condition (i.e., reduction of the Karnofsky performance index < 60%, progression or development of new neurological symptoms, and/or subsequent cancer-related death) as well as progression

in size on contrast-enhanced MRI during follow-up (median follow-up time, 3 months; range, 2-5 months), recurrent BM were diagnosed in 9 patients. In one patient, BM recurrence was diagnosed neuropathologically.

Comparison of Static and Dynamic ^{18}F-FET PET Parameters in Recurrent Brain Metastases and Treatment-related Changes

TBR_{mean} values were significantly higher in patients with BM relapse (n=10) than in patients with treatment-related changes (n=17) (2.4 ± 0.8 vs. 1.7 ± 0.3, $P < 0.001$) (Figure 1). In contrast, TTP values were not significantly different between patients with BM relapse and treatment-related changes (27.7 ± 15.3 minutes vs. 34.5 ± 5.0 minutes, $P = 0.206$). TBR_{mean} and TTP values of each individual patient are listed in Supplemental Table 4.

Diagnostic Perfomance of the Parameters TBR_{mean} and TTP

The ROC analyis revealed that the diagnostic accuracy of TBR_{mean} for the correct identification of recurrent BM reached 85% (AUC, 0.85 ± 0.09; sensitivity, 70%; specificity, 94%; cut-off, 1.95; $P = 0.003$). In contrast, the ROC analysis of the dynamic ^{18}F-FET PET parameter TTP yielded a lower diagnostic performance for the correct identification of recurrent BM (AUC, 0.61 ± 0.18; sensitivity, 100%; specificity, 57%; cut-off, 27.5 minutes; $P = 0.464$). For the diagnosis of BM relapse, presence of a $TBR_{mean} > 1.95$ in combination with a TTP value < 27.5 minutes did not further increase the diagnostic performance (accuracy, 82%; sensitivity, 57%; specificity, 100%; $P = 0.015$).

Assessment of Treatment Response

In 13 patients, ^{18}F-FET PET was performed for the assessement of response to a treatment regimen including ICI or TT using baseline and follow-up ^{18}F-FET PET scans (median time between scans, 4.2 months). Nine of these 13 patients (69%) had ICI or a TT concurrent to radiotherapy (applied within the first 4 weeks after radiotherapy initiation). A detailed overview on the pretreatment and the applied treatment is shown in Supplemental Table 3.

ROC analysis revealed that at follow-up a relative reduction of the TBR_{mean} of 10% or more separated metabolic ^{18}F-FET PET responders (n=6) with a stable clinical course of at least 6 months or more (median follow-up time, 10.5 months; range, 6-18 months) from non-responders with a stable clinical course < 6 months (n=5; median follow-up time, 4 months; range, 2-5 months) with a sensitivity of 80%, a specificity of 83%, and an accuracy of 82% (AUC, 0.78 ± 0.12; P = 0.121). Two of 13 patients examined for the evaluation of treatment response using ^{18}F-FET PET had to be excluded from ROC analysis (loss to follow-up in one patient, death related to other causes than cancer in the other patient). Additionally, metabolic responders on ^{18}F-FET PET (relative reduction of TBR_{mean}, ≥ 10%) had a sigificantly longer stable clinical course than non-responding patients (median time, 10.5 vs. 4 months; P = 0.004).

Furthermore, in metabolic ^{18}F-FET PET responders, TTP values at follow-up increased significantly relative to the baseline TTP values (22.0 ± 9.7 minutes vs. 36.7 ± 5.2 minutes, P = 0.019). In contrast, ^{18}F-FET PET metabolic non-responders showed at follow-up a significant decrease of TTP values (23.0 ± 11.0 minutes vs. 3.4 ± 1.3 minutes,

P = 0.013). TBR_{mean} and TTP values of each individual patient are listed in Supplemental Table 5.

^{18}F-FET PET Findings of Metabolic Responders and Non-Responders in Relation to MRI

In 4 of 13 patients (31%), ^{18}F-FET PET findings at follow-up were discrepant to the changes of contrast-enhanced MRI (Supplemental Table 3). In these cases, ^{18}F-FET PET provided additional information for treatment response evaluation beyond the information provided by contrast-enhanced MRI alone. In particular, ^{18}F-FET PET in two metabolic responders (patient #1 and #8; Supplemental Table 3, 5) showed a significant decrease of metabolic activity (TBR_{mean}, -28% and -15%, respectively), although MRI changes were consistent with progression according to RANO criteria (Figure 2). Furthermore, in contrast to a patient (patient #3; Supplemental Table 3, 5) with unchanged MRI ("Stable Disease" according to RANO criteria) at follow-up, the ^{18}F-FET PET indicated a metabolic response with a significant decline of the TBR_{mean} (-19%). Moreover, although one patient had lesions with increasing metabolic activity (metabolic non-responder; TBR_{mean} increase, 10%), the corresponding MRI suggested even a "partial response" according to RANO criteria (patient #9; Supplemental Table 3, 5) (Figure 3).

DISCUSSION

The main finding of the present study is that ^{18}F-FET PET seems to be of great value for the differentiation of treatment-related changes predominantly induced by ICI or TT in combination with radiotherapy from BM relapse in patients with MM or NSCLC. The

high diagnostic accuracy (85%) could be obtained by a simple and easily applicable approach (i.e., calculation of tumor-to-brain ratios) which facilitates the implementation in clinical routine. This finding is of eminent interest since the combination of radiotherapy with immunotherapy or TT may substantially increase the risk for treatment-related changes such as radiation necrosis (*10,28-31*). Another important finding of our study is the observation that static and dynamic ^{18}F-FET PET parameters may be helpful for the identification of both responders and non-responders to a treatment regimen including ICI or TT with a similar high diagnostic performance (range of accuracy, sensitivity, and specificity, 80-83%). Importantly, metabolic ^{18}F-FET PET responders exhibited a significantly longer stable clinical course during the follow-up than metabolic non-responders (median time, 10.5 vs. 4 months). Moreover, ^{18}F-FET PET provided additional important clinical information for treatment response evaluation beyond the information provided by contrast-enhanced MRI alone, i.e., in terms of identification of false-positive or false-negative MRI findings. Since radiotherapy, immunotherapy with ICI, or TT - especially in combination - play an increasingly important role in personalized treatment of BM, diagnostic information obtained from ^{18}F-FET PET may be therefore of value for patient management. In particular, supplemental ^{18}F-FET PET in cases of ambiguous MRI findings is advantageous for treatment monitoring, providing neurooncologists with a longer time window for subsequent patient management.

Our findings are in line with a small pilot study which highlighted for the first time the potential of ^{18}F-FET PET to identify pseudoprogression in patients with BM originating from MM treated with ICI (*32*). In relation to previous studies evaluating the accuracy of amino acid PET for the diagnosis of treatment-related changes in patients with BM treated

solely with radiotherapy (predominantly radiosurgery), our results are also comparable. These studies using various radiolabeled amino acids including ^{18}F-FET consistently revealed that the sensitivity and specificity for the differentiation of treatment-related changes from BM relapse is in the range of 80-90% (*24,33-40*). Additonally, parameters obtained from dynamic ^{18}F-FET PET acquisition seem to further increase the diagnostic performance compared to static parameters alone (*24,34,38*).

However, in the patients of our study treated with ICI or TT plus radiotherapy (in the majority of patients), the dynamic ^{18}F-FET PET parameter TTP was not able to further improve the diagnostic accuracy in terms of the differentiation between treatment-related changes and BM relapse. Most probably, this is related to the relatively low number of patients available for dynamic data evaluation. Conversely, a recent study suggested that the dynamic ^{18}F-FET PET parameter TTP might be helpful for the differentiation of pseudoprogression from BM relapse in NSCLC patients (n=11) who underwent radiotherapy in combination with ICI (*41*). In that study, however, both the low number (range, 5-8 frames) and the long duration of time frames (5 minutes each) of the applied dynamic PET scanning protocol do not allow a meaningful analysis of ^{18}F-FET uptake over the time, especially in the early phase of dynamic PET acquisition (i.e., 0-20 minutes post-injection).

Notwithstanding, regarding the assessment of response to a treatment regimen including ICI or TT, we observed that the change of the dynamic parameter TTP at follow-up PET imaging seems to be of value to identify both metabolic responders and non-responders. Furthermore, the observed decline of metabolic activity as assessed by TBRs

in responding patients (at least 10% or more compared to baseline imaging), which was associated with a significantly longer stable follow-up, is similar to glioblastoma patients who had a metabolic ^{18}F-FET PET response to chemoradiation with temozolomide (*42*).

Taken together, our findings highlight that newer treatment options have requirements on neuroimaging which cannot be met by conventional MRI. Non-amino acid PET tracers seem also to be of value for treatment monitoring of these newer treatment options for patients with BM. For example, the tracer 3′-deoxy-3′-[^{18}F]fluorothymidine (^{18}F-FLT), an analog to the nucleoside thymidine and a marker for cellular proliferation, was used in BM patients secondary to MM treated with immunotherapy using ICI or TT (*43*). It could be observed that responding patients may show a more pronounced proliferative reduction on ^{18}F-FLT PET than the reduction of contrast enhancement on standard MRI.

Nevertheless, the present study has several limitations. Due to its retrospective nature, the findings should be interpreted with caution and our results warrant confirmation by a prospective study. One might argue that the number of included patients is relatively low. Nevertheless, our dataset includes the highest number of patients treated with ICI or TT, predominantly with radiotherapy, who were monitored with ^{18}F-FET PET (in part even with serial scans), allowing a more profound evaluation of this clinically promising imaging technique. Another putative weakness is the heterogeneity of the applied treatment. Apart from clinical trials this represents a “real life” constellation in many brain tumor centers and reflects also the current concept of personalized medicine in cancer patients. Furthermore, because multiple lesions occurred frequently and tissue for neuropathological evaluation obtained by biopsy was not available, radiological/clinical

criteria had to be used for the final diagnosis in the majority of the lesions. However, in clinical routine ethical issues or medical contraindications influence not infrequently the indication for a biopsy. Since alternative diagnostic methods such as liquid biopsy are clinically not yet established, the assessment of response by radiological/clinical criteria is a reasonable alternative.

In conclusion, our findings suggest that ^{18}F-FET PET is a useful method in clinically challenging situations, especially when conventional MRI is equivocal. The detection of BM relapse with high accuracy as well as the reliable assessment of response is essential for optimizing patient counseling as well as the treatment concept for each individual patient. Furthermore, this approach achieves an accuracy that is sufficient to influence clinical decision-making and may therefore help to reduce the number of invasive diagnostic interventions and overtreatment for a considerable number of seriously ill patients with BM. A larger prospective study is warranted to confirm the clinical usefulness of ^{18}F-FET PET-derived imaging parameters for treatment monitoring of regimens which include newer treatment options such as ICI or TT.

COMPETING INTERESTS

The authors declare that they have no competing interests.

ETHICS APPROVAL AND CONSENT TO PARTICIPATE

All subjects gave prior written informed consent for their participation in the ^{18}F-FET PET study and evaluation of their data for scientific purposes. The local ethics committee approved the evaluation of retrospectively collected patient data. All procedures

performed in studies involving human participants followed the national ethical standards and the Declaration of Helsinki.

KEY POINTS

- Amino acid PET using the tracer O-(2-[^{18}F]fluoroethyl)-L-tyrosine **(**FET) may add valuable information for the diagnosis of treatment-related changes in BM patients undergoing immune checkpoint inhibition or targeted therapy alone or in combination with radiotherapy

- ^{18}F-FET PET helps to identify responders to radiotherapy in combination with checkpoint inhibitors or targeted therapy

- Conventional MRI findings can be discrepant (i.e., unchanged or even progressive) in ^{18}F-FET PET responders

- Responding patients on ^{18}F-FET PET had a significantly longer stable clinical course of 6 months or more

REFERENCES

1. Soffietti R, Abacioglu U, Baumert B, et al. Diagnosis and treatment of brain metastases from solid tumors: guidelines from the European Association of Neuro-Oncology (EANO). *Neuro Oncol.* 2017;19:162-174.

2. Reck M, Rodriguez-Abreu D, Robinson AG, et al. Pembrolizumab versus chemotherapy for PD-L1-positive non-small-cell lung cancer. *N Engl J Med.* 2016;375:1823-1833.

3. Borghaei H, Paz-Ares L, Horn L, et al. Nivolumab versus docetaxel in advanced nonsquamous non-small-cell lung cancer. *N Engl J Med.* 2015;373:1627-1639.

4. Flaherty KT, Infante JR, Daud A, et al. Combined BRAF and MEK inhibition in melanoma with BRAF V600 mutations. *N Engl J Med.* 2012;367:1694-1703.

5. Long GV, Atkinson V, Lo S, et al. Combination nivolumab and ipilimumab or nivolumab alone in melanoma brain metastases: a multicentre randomised phase 2 study. *Lancet Oncol.* 2018;19:672-681.

6. Wu YL, Ahn MJ, Garassino MC, et al. CNS efficacy of osimertinib in patients with T790M-positive advanced non-small-cell lung cancer: Data from a randomized phase III trial (AURA3). *J Clin Oncol.* 2018;36:2702-2709.

7. Tawbi HA, Forsyth PA, Algazi A, et al. Combined nivolumab and ipilimumab in melanoma metastatic to the brain. *N Engl J Med.* 2018;379:722-730.

8. Davies MA, Saiag P, Robert C, et al. Dabrafenib plus trametinib in patients with BRAF(V600)-mutant melanoma brain metastases (COMBI-MB): a multicentre, multicohort, open-label, phase 2 trial. *Lancet Oncol.* 2017;18:863-873.

9. Okada H, Weller M, Huang R, et al. Immunotherapy response assessment in neuro-oncology: a report of the RANO working group. *Lancet Oncol.* 2015;16:e534-542.

10. Galldiks N, Kocher M, Ceccon G, et al. Imaging challenges of immunotherapy and targeted therapy in patients with brain metastases: response, progression, and pseudoprogression. *Neuro Oncol.* 2020;22:17-30.

11. Cohen JV, Alomari AK, Vortmeyer AO, et al. Melanoma brain metastasis pseudoprogression after pembrolizumab treatment. *Cancer Immunol Res.* 2016;4:179-182.

12. Langen KJ, Galldiks N, Hattingen E, Shah NJ. Advances in neuro-oncology imaging. *Nat Rev Neurol.* 2017;13:279-289.

13. Okubo S, Zhen HN, Kawai N, Nishiyama Y, Haba R, Tamiya T. Correlation of L-methyl-11C-methionine (MET) uptake with L-type amino acid transporter 1 in human gliomas. *J Neurooncol.* 2010;99:217-225.

14. Youland RS, Kitange GJ, Peterson TE, et al. The role of LAT1 in (18)F-DOPA uptake in malignant gliomas. *J Neurooncol.* 2013;111:11-18.

15. Papin-Michault C, Bonnetaud C, Dufour M, et al. Study of LAT1 expression in brain metastases: towards a better understanding of the results of positron emission tomography using amino acid tracers. *PLoS One.* 2016;11:e0157139.

16. Albert NL, Weller M, Suchorska B, et al. Response Assessment in Neuro-Oncology working group and European Association for Neuro-Oncology recommendations for the clinical use of PET imaging in gliomas. *Neuro Oncol.* 2016;18:1199-1208.

17. Galldiks N, Langen KJ, Albert NL, et al. PET imaging in patients with brain metastasis-report of the RANO/PET group. *Neuro Oncol.* 2019;21:585-595.

18. Law I, Albert NL, Arbizu J, et al. Joint EANM/EANO/RANO practice guidelines/SNMMI procedure standards for imaging of gliomas using PET with radiolabelled amino acids and [(18)F]FDG: version 1.0. *Eur J Nucl Med Mol Imaging.* 2019;46:540-557.

19. Ellingson BM, Bendszus M, Boxerman J, et al. Consensus recommendations for a standardized Brain Tumor Imaging Protocol in clinical trials. *Neuro Oncol.* 2015;17:1188-1198.

20. Lin NU, Lee EQ, Aoyama H, et al. Response assessment criteria for brain metastases: proposal from the RANO group. *Lancet Oncol.* 2015;16:e270-278.

21. Hamacher K, Coenen HH. Efficient routine production of the 18F-labelled amino acid O-2-18F fluoroethyl-L-tyrosine. *Appl Radiat Isot.* 2002;57:853-856.

22. Herzog H, Langen KJ, Weirich C, et al. High resolution BrainPET combined with simultaneous MRI. *Nuklearmedizin.* 2011;50:74-82.

23. Pauleit D, Floeth F, Hamacher K, et al. O-(2-[18F]fluoroethyl)-L-tyrosine PET combined with MRI improves the diagnostic assessment of cerebral gliomas. *Brain.* 2005;128:678-687.

24. Ceccon G, Lohmann P, Stoffels G, et al. Dynamic O-(2-18F-fluoroethyl)-L-tyrosine positron emission tomography differentiates brain metastasis recurrence from radiation injury after radiotherapy. *Neuro Oncol.* 2017;19:281-288.

25. Langen KJ, Bartenstein P, Boecker H, et al. [German guidelines for brain tumour imaging by PET and SPECT using labelled amino acids]. *Nuklearmedizin.* 2011;50:167-173.

26. Kinahan PE, Fletcher JW. Positron emission tomography-computed tomography standardized uptake values in clinical practice and assessing response to therapy. *Semin Ultrasound CT MR.* 2010;31:496-505.

27. Galldiks N, Stoffels G, Filss C, et al. The use of dynamic O-(2-18F-fluoroethyl)-l-tyrosine PET in the diagnosis of patients with progressive and recurrent glioma. *Neuro Oncol.* 2015;17:1293-1300.

28. Kroeze SG, Fritz C, Hoyer M, et al. Toxicity of concurrent stereotactic radiotherapy and targeted therapy or immunotherapy: A systematic review. *Cancer Treat Rev.* 2017;53:25-37.

29. Fang P, Jiang W, Allen P, et al. Radiation necrosis with stereotactic radiosurgery combined with CTLA-4 blockade and PD-1 inhibition for treatment of intracranial disease in metastatic melanoma. *J Neurooncol.* 2017;133:595-602.

30. Trommer-Nestler M, Marnitz S, Kocher M, et al. Robotic stereotactic radiosurgery in melanoma patients with brain metastases under simultaneous anti-PD-1 treatment. *Int J Mol Sci.* 2018;19.

31. Galldiks N, Lohmann P, Werner JM, Ceccon G, Fink GR, Langen KJ. Molecular imaging and advanced MRI findings following immunotherapy in patients with brain tumors. *Expert Rev Anticancer Ther.* 2020;20:9-15.

32. Kebir S, Rauschenbach L, Galldiks N, et al. Dynamic O-(2-[18F]fluoroethyl)-L-tyrosine PET imaging for the detection of checkpoint inhibitor-related pseudoprogression in melanoma brain metastases. *Neuro Oncol.* 2016;18:1462-1464.

33. Terakawa Y, Tsuyuguchi N, Iwai Y, et al. Diagnostic accuracy of 11C-methionine PET for differentiation of recurrent brain tumors from radiation necrosis after radiotherapy. *J Nucl Med.* 2008;49:694-699.

34. Galldiks N, Stoffels G, Filss CP, et al. Role of O-(2-18F-fluoroethyl)-L-tyrosine PET for differentiation of local recurrent brain metastasis from radiation necrosis. *J Nucl Med.* 2012;53:1367-1374.

35. Lizarraga KJ, Allen-Auerbach M, Czernin J, et al. (18)F-FDOPA PET for differentiating recurrent or progressive brain metastatic tumors from late or delayed radiation injury after radiation treatment. *J Nucl Med.* 2014;55:30-36.

36. Cicone F, Minniti G, Romano A, et al. Accuracy of F-DOPA PET and perfusion-MRI for differentiating radionecrotic from progressive brain metastases after radiosurgery. *Eur J Nucl Med Mol Imaging.* 2015;42:103-111.

37. Minamimoto R, Saginoya T, Kondo C, et al. Differentiation of brain tumor recurrence from post-radiotherapy necrosis with 11C-Methionine PET: visual assessment versus quantitative assessment. *PLoS One.* 2015;10:e0132515.

38. Romagna A, Unterrainer M, Schmid-Tannwald C, et al. Suspected recurrence of brain metastases after focused high dose radiotherapy: can [18F]FET-PET overcome diagnostic uncertainties? *Radiat Oncol.* 2016;11:139.

39. Yomo S, Oguchi K. Prospective study of (11)C-methionine PET for distinguishing between recurrent brain metastases and radiation necrosis: limitations of diagnostic accuracy and long-term results of salvage treatment. *BMC Cancer.* 2017;17:713.

40. Lohmann P, Kocher M, Ceccon G, et al. Combined FET PET/MRI radiomics differentiates radiation injury from recurrent brain metastasis. *Neuroimage Clin.* 2018;20:537-542.

41. Akhoundova D, Hiltbrunner S, Mader C, et al. 18F-FET PET for Diagnosis of pseudoprogression of brain metastases in patients with non-small cell lung cancer. *Clin Nucl Med.* 2020;45:113-117.

42. Galldiks N, Langen K, Holy R, et al. Assessment of treatment response in patients with glioblastoma using [18F]Fluoroethyl-L-Tyrosine PET in comparison to MRI. *J Nucl Med.* 2012;53:1048-1057.

43. Nguyen NC, Yee MK, Tuchayi AM, Kirkwood JM, Tawbi H, Mountz JM. Targeted therapy and immunotherapy response assessment with F-18 fluorothymidine Positron-Emission Tomography/Magnetic Resonance Imaging in melanoma brain metastasis: a pilot study. *Front Oncol.* 2018;8:18.

Figure 1

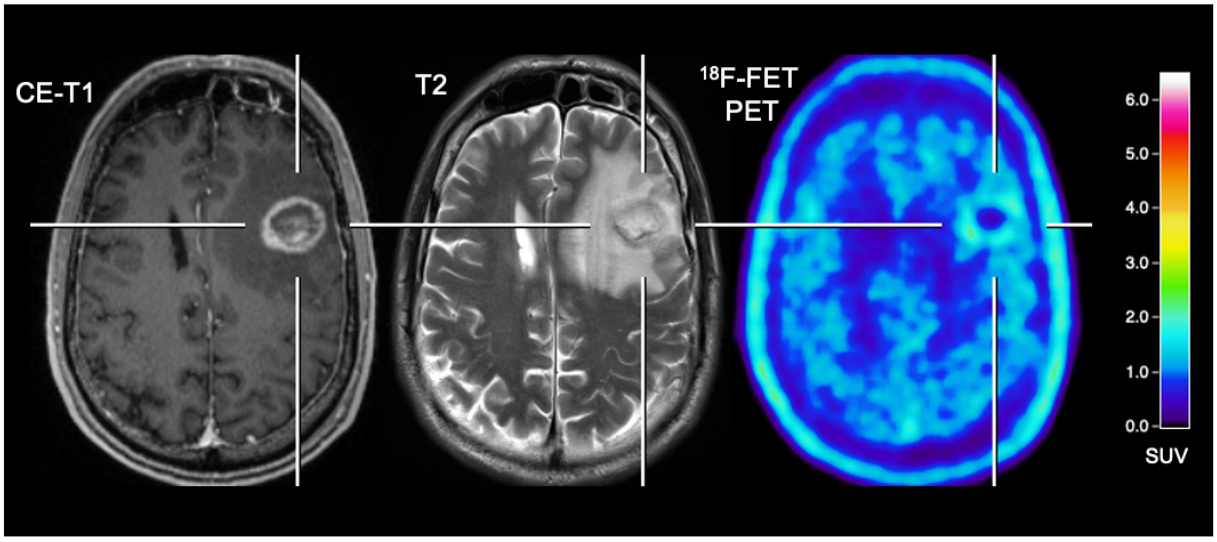

Figure 1: Patient with a melanoma brain metastasis pretreated with radiosurgery concurrent with nivolumab, and dabrafenib in combination with trametinib (patient #9; Supplemental Table 2, 4). In contrast to the progressive MRI, amino acid PET using ^{18}F-FET shows no significant uptake and is consistent with treatment-related changes. After PET imaging, the survival time was 24 months.

Figure 2

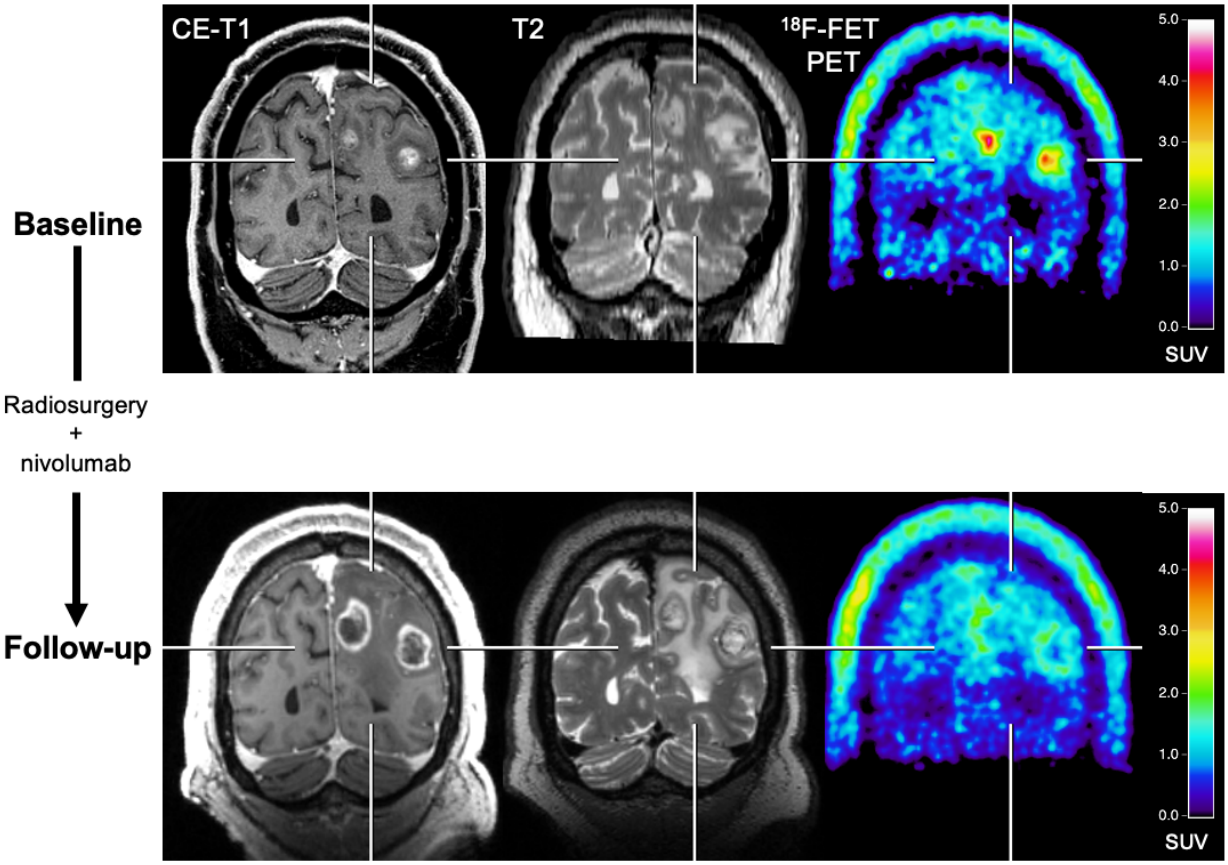

Figure 2: Following radiosurgery concurrent to nivolumab in a 59-year-old patient with melanoma brain metastases (patient #1; Supplemental Table 3, 5), ^{18}F-FET PET at follow-up 12 weeks after treatment initiation (bottom row) shows a significant decrease of metabolic activity (TBR_{mean}, -28%) compared to baseline (top row), although MRI changes were consistent with progression according to RANO criteria. The reduction of metabolic activity was associated with a stable clinical course over 10 months.

Figure 3

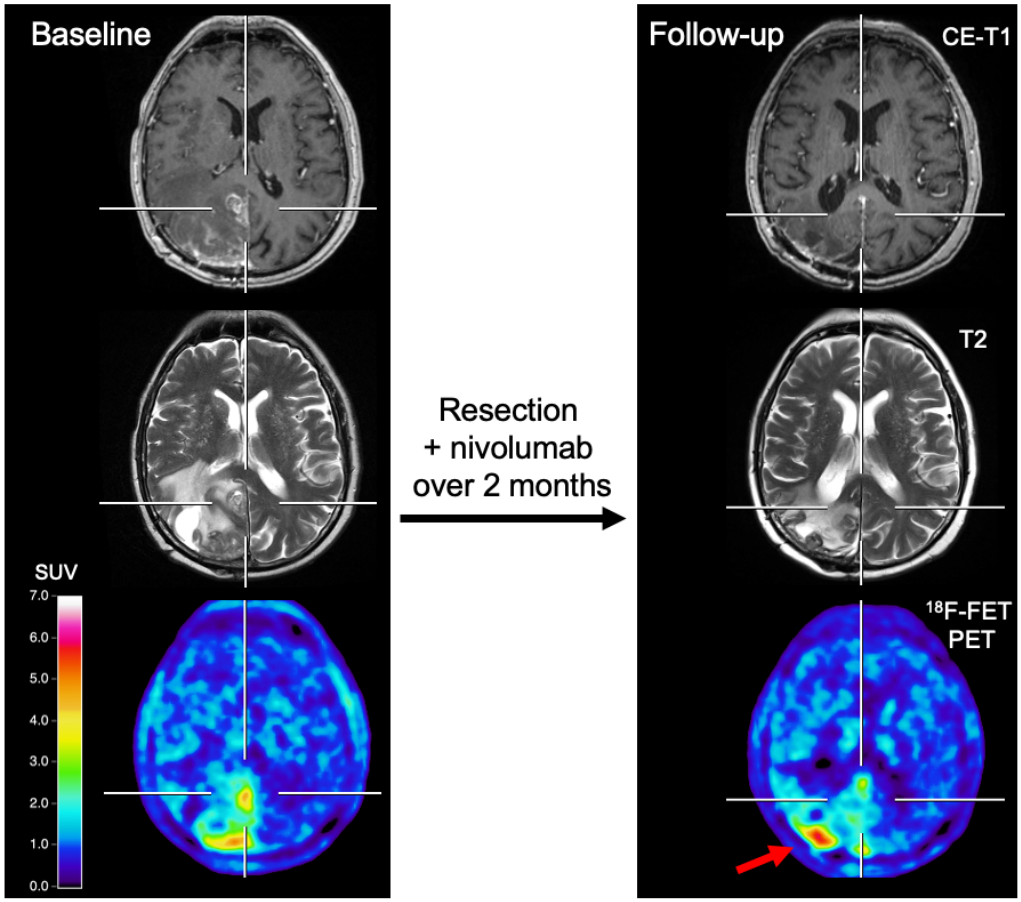

Figure 3: 67-year-old patient with multiple brain metastasis secondary to a non-small cell lung cancer treated with surgery followed by nivolumab (patient #9; Supplemental Table 3, 5). ^{18}F-FET PET at follow-up is consisted with a “mixed response”. Besides reduction of metabolic activity in some lesions, especially the right occipital lesion shows increasing metabolic activity (TBR_{mean} increase, 10%). In contrast, the corresponding MRI suggested “partial response” according to RANO criteria. The patient died two months later.

Supplemental Table 1: Overview of targeted and checkpoint inhibitor therapy in relation to radiotherapy to the brain and timing of FET PET imaging

	Number of patients	Radiosurgery (n patients)	WBRT (n patients)	Radiosurgery and WBRT (n patients)	Other radiotherapy types* (n patients)
RT pretreatment only prior to FET PET	14 (35%)	4	3	3	4
RT pretreatment plus ICI or TT prior to FET PET	14 (35%)	10	2	1	1
ICI or TT concurrent to RT and PET***	9 (22.5%)	6	2	0	1
	37 (92.5%)	20 (50%)	7 (17.5%)	4 (10%)	6 (15%)
No RT during the course of disease (ICI or TT only)	3 (7.5%)	n.a.	n.a.	n.a.	n.a.
	40 (100%)				

ICI = immune checkpoint inhibition; **n.a.** = not available; **RT** = radiotherapy; **TT** = targeted therapy; **WBRT** = whole-brain radiotherapy; * = external fractionated radiotherapy (n=5), brachytherapy (n=1); ** = ICI or TT applied within the first 4 weeks after radiotherapy initiation; *** = patients examined for treatment response assessment

Supplemental Table 2: Overview of the patients examined using FET PET for the differentiation of treatment-related changes from brain metastasis relapse

Patient #	Gender, age (years) at diagnosis of the primary tumor	Pathological diagnosis and molecular characteristics of the primary tumor	Number of BM on MRI at initial diagnosis	BM pretreatment before PET imaging	Applied BM treatment concurrent to FET PET	Time between BM treatment initiation and first FET PET (mo)	Number of FET PET scans	FET PET findings	FET PET findings consistent with BM relapse?	Confirmation of FET PET findings	Final diagnosis
1	M, 40	MM	1	ipi	SRS + pembro	3	3	no increased MA	no	stable FU, 25 mo	TRC
2	M, 26	MM	2	n.a.	SRS + nivo	5	3	no increased MA in 1 BM increased MA in 1 BM	yes	histologically	BM relapse
3	M, 65	NSCLC	3	SRS	SRS + nivo	7	2	no increased MA	no	stable FU, 7 mo	TRC
4	F, 52	NSCLC	3	SRS	pembro	2	1	no increased MA	no	stable FU, 8 mo	TRC
5	M, 63	MM, BRAF mut	2	SRS, dabra + tram, WBRT, ipi + nivo	vemura	30	1	no increased MA	no	died 4 mo later	BM relapse
6	M, 77	MM, BRAF mut	2	SRS + nivo	n.a.	28	1	no increased MA	no	stable FU, 11 mo	TRC
7	M, 44	MM, BRAF mut	2	WBRT	dabra + tram	4	1	increased MA in 2 BM	yes	died 2 mo later	BM relapse
8	M, 54	MM, BRAF mut, PD-L1 expression <5%	2	n.a.	dabra + tram	1	1	no increased MA	no	stable FU, 7 mo	TRC

9	M, 35	MM, BRAF mut	2	R, SRS + nivo	dabra + tram	11	1	no increased MA	no	died 24 mo later	TRC
10	M, 75	MM	1	n.a.	SRS + nivo	7	1	no increased MA	no	stable FU, 7 mo	TRC
11	M, 66	MM, BRAF mut	4	WBRT, dabra + tram	ipi	12	1	increased MA in all 4 BM	yes	died 5 mo later	BM relapse
12	M, 50	MM, BRAF wt	3	R, WBRT	ipi	12	1	no increased MA	no	stable FU, 6 mo	TRC
13	M, 24	NSCLC, ROS transl, EGFR wt, PD-L1 expression 5-10%	2	R, RT, SRS	criz	6	2	no increased MA	no	histologically confirmed RN	TRC
14	M, 51	NSCLC	3	WBRT, SRS	nivo	38	1	increased MA	yes	treatment change	BM relapse
15	F, 51	NSCLC	1	WBRT	criz	13	1	no increased MA	no	stable FU, 22 mo	TRC
16	F, 66	MM, BRAF wt	1	n.a.	ipi	4	1	increased MA	yes	treatment change	BM relapse
17	M, 57	NSCLC	6	SRS	nivo	12	1	increased MA in 1 of 3 BM	yes	treatment change	BM relapse
18	M, 61	NSCLC	1	WBRT, SRS	nivo	18	1	no increased MA	no	stable FU, 19 mo	TRC
19	M, 56	MM, BRAF wt, NRAS mut	2	R, SRS, ipi	none	14	1	no increased MA	yes	MRI improvement 3 mo later	TRC
20	M, 52	MM, BRAF mut	3	R, SRS, ipi + nivo	nivo	10	1	increased MA	no	MRI 3 mo later shows SD	TRC
21	M, 34	MM, BRAF wt, NRAS mut	2	R, SRS, bini, ipi, pembro	pembro	36	1	no increased MA	no	MRI improvement 3 mo later	TRC
22	M, 55	MM, BRAF wt, NRAS mut	17	WBRT,ipi + nivo	nivo	10	1	no increased MA	no	MRI improvement 3 mo later	TRC
23	M, 60	MM, BRAF wt, NRAS mut, PD-L1 2%	1	SRS, pembro, ipi	bini	17	1	no increased MA	no	MRI 3 mo later showns SD	TRC
24	M, 57	MM, BRAF mut	1	SRS, nivo	n.a.	2	1	no increased MA	no	MRI 3 mo later shows SD	TRC

25	M, 56	MM, BRAF mut, NRAS wt, PD-L1 0%	2	R, ipi + nivo, SRS	nivo	8	1	no increased MA	no	MRI 3 mo later PD	BM relapse
26	M, 72	MM, BRAF wt, NRAS mut	4	R, RT, SRS, ipi + nivo	none	17	1	no increased MA	no	MRI 3 mo later PD	BM relapse
27	M, 55	MM, BRAF mut, NRAS wt	1	R, ipi + nivo	RT, ipi + nivo	1	1	increased MA	no	leptomeningeal metastases 3 mo later	BM relapse

bini = binimetinib; **BM** = brain metastases; **CE** = contrast enhancement; **criz** = crizotinib; **decrease of MA** = significant decrease of metabolic activity as indicated by a decline of the mean tumor-to-brain ratio of ≥ 10% compared to the baseline FET PET image **dabra** = dabrafenib; **F** = female; **FU** = follow-up; **increased MA** = metabolic activity as assessed by a mean tumor-to-brain ratio ≥ 2.0; **ipi** = ipilimumab; **M** = male; **MA** = metabolic activity; **MM** = malignant melanoma; **mo** = months; **mut** = mutant; **n.a.** = not available; **NSCLC** = non-small cell lung cancer; **nivo** = nivolumab; **no increased MA** = metabolic activity as assessed by a mean tumor-to-brain ratio < 2.0; **pembro** = pembrolizumab; **PD** = progressive disease according to RANO criteria for brain metastases; **PR** = partial response according to RANO criteria for brain metastases; **R** = resection; **RN** = radiation necrosis; **RT** = external fractionated radiotherapy; **SRS** = stereotactic radiosurgery; **tram** = trametinib; **transl** = translocation; **TRC** = treatment-related changes; **vemura** = vemurafenib; **WBRT** = whole-brain radiation therapy; **wt** = wildtype

Supplemental Table 3: Overview of the patients examined using FET PET for the assessment of treatment response

Patient #	Gender, age (years) at diagnosis of the primary tumor	Pathological diagnosis and molecular characteristics of the primary tumor	Number of BM on MRI at baseline	BM pretreatment before PET imaging	Applied BM treatment evalued for response using FET PET	Number of FET PET scans	Baseline FET PET findings	First follow-up FET PET findings	Second follow-up FET PET findings	FET PET consistent with response?	FET PET discrepant to MRI findings at follow-up?	Confirmation of FET PET findings
1	M, 59	MM, BRAF mut, no PD-L1 expression	3	n.a.	SRS + nivo	3	increased MA in all 3 BM	decrease of MA in all 3 BM detection of 1 new BM with increased MA	after SRS decrease of MA in the new BM	yes	yes, MRI consistent with PD	stable FU, 10 mo
2	F, 56	NSCLC, EGFR mut, no PD-L1 expression	4	n.a.	WBRT + afa	2	increased MA in 1 of 4 BM	decrease of MA	n.a.	yes	no	stable FU, 11 mo
3	F, 36	MM, BRAF mut	3	R + RT	dabra + tram	2	increased MA in all 3 BM	decrease of MA in 2 of 3 BM unchanged MA in 1 BM	n.a.	yes	yes, MRI unchanged	stable FU, 6 mo
4	M, 69	MM, BRAF mut	6	n.a.	dabra + tram	2	increased MA in 3 of 6 BM	decrease of MA in 1 of 3 BM unchanged MA in 2 BM	n.a.	no	no	died 4 mo later
5	F, 78	MM, BRAF mut	1	n.a.	SRS + pembro	2	increased MA in 1 BM	insignificant decrease of MA	n.a.	no	no	died 5 mo later
6	M, 73	MM, BRAF wt, NRAS WT	1	n.a.	SRS + pembro	2	increased MA in 1 BM	decrease of MA	n.a.	yes	no	intra- and extracranial PD after stable FU of 4 mo
7	F, 45	MM, BRAF wt	1	n.a.	SRS + pembro	2	increased MA in 1 BM	decrease of MA	n.a.	yes	no	stable FU, 15 mo

8	M, 76	MM	2	SRS, WBRT	dabra + tram	2	increased MA in 1 BM	decrease of MA	n.a.	yes	yes, MRI consistent with PD	lost of follow-up
9	M, 67	NSCLC	3	R, SRS	R, nivo	2	increased MA in all 3 BM	further increase of MA in one BM	n.a.	no	yes, MRI consistent with PR	died 2 mo later
10	M, 28	MM, BRAF mut	1	SRS, pembro	SRS + dabra + tram	2	increased MA	further increase of MA	n.a.	no	no	died 2 mo later
11	M, 58	NSCLC, PD-L1 expression 5%	1	R + RT, SRS	brachy + nivo	3	increased MA	decrease of MA	decrease of MA	yes	no	died 10 mo later due to extracranial PD
12	F, 51	MM	2	RT	WBRT + nivo	2	increased MA	decrease of MA	n.a.	yes	no	died 18 mo later
13	M, 59	NSCLC, TP53 mutation PD-L1 expression > 50%	5	n.a.	SRS + pembro	2	no increased MA	no increased MA	n.a.	yes	no	died 1 mo later, dead not cancer-related

afa = afatinib; **BM** = brain metastases; **decrease of MA** = significant decrease of metabolic activity as indicated by a decline of the mean tumor/brain ratio of ≥ 10% compared to the baseline FET PET image; **dabra** = dabrafenib; **F** = female; **increased MA** = metabolic activity as assessed a mean tumor-to-brain ratio of ≥ 2.0; **ipi** = ipilimumab; **M** = male; **MA** = metabolic activity; **MM** = malignant melanoma; **mo** = month(s); **mut** = mutant; **n.a.** = not available; **nivo** = nivolumab; **NSCLC** = non-small cell lung cancer; **PD** = progressive disease; **pembro** = pembrolizumab; **PR** = partial response according to the RANO criteria for brain metastases; **R** = resection; **SRS** = stereotactic radiosurgery; **RT** = external fractionated radiotherapy; **tram** = trametinib; **WBRT** = whole-brain radiation therapy; **wt** = wildtype

Supplemental Table 4: Overview of FET PET findings for the differentiation of treatment-related changes from brain metastasis relapse

Patient #	Number of FET PET lesions	TBR_{mean} values at suspected relapse	TTP values at suspected relapse (minutes)	TBR_{mean} values on additional FET PET scan(s) during follow-up	Final diagnosis
1	1	1.6	45	scan #1: 1.6 scan #2: 1.6	TRC
2	2	2.2 / 1.7	25	scan #1: no uptake (resection cavity) / 1.7 scan #2: 2.7 (new lesion)	BM relapse
3	1	1.0	n.d.	1.0	TRC
4	1	1.8	30	n.a.	TRC
5	3	1.9 / 1.8 / 1.7	45	n.a.	BM relapse
6	1	1.8	30	n.a.	TRC
7	2	2.6 / 2.3	45	n.a.	BM relapse
8	1	1.7	35	n.a.	TRC
9	1	1.7	35	n.a.	TRC
10	2	1.9 / 1.8	30	n.a.	TRC
11	4	4.5 / 2.6 / 2.2 / 2.0	13	n.a.	BM relapse
12	3	1.8 / 1.7 / 1.7	40	n.a.	TRC
13	1	1.6	35	scan #1: 1.9 (new lesion)	TRC
14	1	2.2	13	n.a.	BM relapse
15	1	1.7	35	n.a.	TRC
16	1	2.8	40	n.a.	BM relapse
17	3	2.3 / 1.9 / 1.7	13	n.a.	BM relapse
18	1	1.9	30	n.a.	TRC
19	1	1.7	n.a.	n.a.	TRC
20	1	2.1	n.a.	n.a.	TRC
21	1	1.0	n.a.	n.a.	TRC
22	1	1.8	n.a.	n.a.	TRC
23	1	1.9	n.a.	n.a.	TRC
24	1	1.5	n.a.	n.a.	TRC
25	1	1.0	n.a.	n.a.	BM relapse
26	1	1.8	n.a.	n.a.	BM relapse
27	1	2.0	n.a.	n.a.	BM relapse

BM = brain metastasis(es); **n.d.** = not determined due to no increased FET uptake; **TBR_{mean}** = mean tumor-to-brain ratio (in the case of multiple lesions, the lesion with the highest metabolic activity has been selected for the analysis of the diagnostic performance); **TRC** = treatment-related changes; **TTP** = time-to-peak (in the case of multiple lesions, the lesion with the highest metabolic activity has been selected for TTP calculation)

Supplemental Table 5: Overview of FET PET findings for the assessment of treatment response

Patient #	Baseline FET PET TBR_{mean}	Baseline TTP (minutes)	Follow-up FET PET (TBR_{mean})	Follow-up TTP (minutes)	Change TBR_{mean} (%)	Stable clinical follow-up (months)
1	2.5	17	1.8	35	-28	10
2	1.9	40	1.7	35	-11	11
3	2.6	25	2.1	40	-19	6
4	2.3	8	2.1	25	-9	died after 4 mo
5	2.0	20	1.9	25	-5	died after 5 mo
6	2.5	5	1.8	35	-28	4
7	2.1	17	1.7	30	-19	15
8	2.0	20	1.7	40	-15	lost of follow-up
9	2.1	8	2.3	5	10	died after 2 mo
10	1.8	30	3.1	25	72	died after 2 mo
11	2.2	13	1.7	35	-23	10
12	1.8	20	1.7	45	-6	18
13	1.0	n.d.	1.0	n.d.	0	died 1 mo later, dead not cancer-related

n.d. = not determined due to no increased FET uptake; **mo** = month(s); **TBR_{mean}** = mean tumor-to-brain ratio (in the case of multiple brain metastases, the lesion with the highest metabolic activity has been selected for TBR_{mean} calculation and response assessment); **TTP** = time-to-peak (in the case of multiple brain metastases, the lesion with the highest metabolic activity has been selected for TTP calculation and response assessment)